Nonenzymatic Glycosylation-induced Modifications of Intact Bovine Kidney Tubular Basement Membrane

Shane S. Anderson, Effie C. Tsilibary, and Aristidis S. Charonis
Department of Laboratory Medicine and Pathology, University of Minnesota Medical School, Minneapolis, Minnesota 55113

Abstract

We examined structural changes in bovine kidney tubular basement membrane (TBM) following in vitro nonenzymatic glycosylation (NEG). Isolated TBM was incubated for 2 wk at 37°C in the absence of sugar or in the presence of either glucose or ribitol under conditions that minimized degradation and oxidative damage. NEG and crosslink formation in glycated TBM were confirmed by decreased solubility, increased amounts of low mobility material by SDS-PAGE, and increased specific fluorescence compared to controls. Morphological analysis using high resolution, low voltage scanning electron microscopy (LV-SEM) revealed a complex three-dimensional meshwork of interconnecting strands with intervening openings. Glycated TBM underwent distinct morphological changes, including a 58% increase in the amount of image surface area occupied by openings. This was due to an apparent increase in the number of large openings (diameters > 12.5 nm), whereas the number of small openings (diameters < 12.5 nm) remained unchanged. These findings corroborate earlier physiological studies, which established that the loss of glomerular permselectivity seen in patients with diabetic nephropathy is due to the formation of large pores in the kidney filtration barrier of which the BM is a major component. We conclude that NEG and crosslink formation among BM components lead to modifications of BM ultrastructure, which could play a role in loss of barrier function in diabetic microangiopathy and nephropathy. (*J. Clin. Invest.* 1993. 92:3045–3052.) Key words: diabetes • microangiopathy • nephropathy • scanning electron microscopy • advanced glycosylation endproducts

Introduction

Basement membranes (BM)[1] are specialized regions of the extracellular matrix composed of type IV collagen (tIV), laminin (LM), entactin/nidogen, and proteoglycans, which together form a complex meshlike structure (1). Found primarily at the basal surface of polarized cells, BM are thought to have several important functions, sievelike permselectivity being one of them. Decreased vascular wall permselectivity is one of several sequelae typical of longstanding diabetes mellitus. This process has been most thoroughly studied in the glomerular filtration barrier of the kidney, composed of a sievelike BM situated between vascular endothelium and urinary epithelium. Ordinarily, this high capacity filter is impermeable to large plasma proteins such as albumin and immunoglobulin. However, a high percentage of diabetic patients show a gradual decline in the permselectivity of the glomerular filtration barrier as detected by progressively increasing proteinuria.

The cause of this decline in permselectivity is unclear. Factors like impaired charge density may contribute to the leakage of negatively charged proteins like albumin; however, Myers and his colleagues have provided evidence that a loss of size selectivity is by far the most crucial element in the development of diabetic nephropathy (2). Based on the transglomerular sieving of uncharged dextran molecules with broad size distribution in normal individuals and in diabetic patients with various degrees of proteinuria, they have modeled the renal filtration barrier as a heteroporous membrane primarily composed of small restrictive pores with a minor component of larger nonrestrictive pores. In this model, a slight increase in the proportion of larger pores is able to account entirely for the altered permselectivity of the diabetic glomerulus (2). Despite changes in glomerular basement membrane (GBM) structure described by Østerby et al. as "fluffiness," which have been correlated with proteinuria (3), the nature of these large pores and the mechanism by which they may form are not well established.

Nonenzymatic glycosylation (NEG) of long-lived proteins, such as the basement membrane components tIV and LM, is one of several mechanisms that may be involved in the generation of diabetic complications. It is a well-described process that becomes highly accelerated in diabetes (4). At the molecular level, NEG begins with the spontaneous and reversible condensation of glucose, a reducing sugar, with a free amino group, usually the ϵ-amino group of a lysine residue. The Schiff base that is formed undergoes Amadori rearrangement and can then condense with an adjacent ketoamine adduct or amino acid side chain to form an irreversible crosslink product (5). Several proteins, including isolated tIV and LM, undergo structural and functional changes after glucose incorporation and/or ensuing protein crosslinking (6–9). However, the effect of NEG on the structural integrity of whole BM has not been addressed so far.

In the present report, using tubular basement membrane (TBM) as a model system, we examined the structural changes

Address correspondence to Dr. Aristidis S. Charonis, Department of Laboratory Medicine and Pathology, University of Minnesota Medical School, Box 609 UMHC, 420 Delaware Street S.E., Minneapolis, MN 55455.

Received for publication 27 May 1993 and in revised form 13 August 1993.

1. *Abbreviations used in this paper:* BM, basement membrane; LM, laminin; LV-SEM, low voltage scanning electron microscopy; NEG, nonenzymatic glycosylation; NEM, *N*-ethylmaleimide; TBM, tubular basement membrane; tIV, type IV collagen.

J. Clin. Invest.

0021-9738/93/12/3045/08 $2.00
Volume 92, December 1993, 3045–3052

that intact isolated BM undergoes after NEG and extensive crosslinking. We have used a novel morphological approach employing ultra high resolution, low voltage scanning electron microscopy (LV-SEM) and computer-aided image analysis to identify these changes.

Methods

Research design. Minimally extracted TBM was isolated from calf kidneys and used as an in vitro model system to assess the influence of glycation on BM ultrastructure. Tissue from young animals was used because a minimal number of preexisting crosslinks are present. TBM was incubated with glucose, a reducing sugar, under conditions resulting in detectable glycation and crosslinking while minimizing protein degradation, oxidation, and bacterial contamination. TBM treated with ribitol, a nonreducing sugar, was used as a control to correct for possible osmotic or other nonspecific influences of high sugar concentration on TBM structure. Following incubation, glycation and crosslinking were confirmed biochemically, and influence of glycation on TBM ultrastructure was examined by LV-SEM and computer-aided image analysis.

Isolation of renal tubules. Renal tubules were isolated from calf kidneys using the technique of Butkowski and Hagen (10). The glomeruli and tubules from this young tissue were isolated on sieves with mesh sizes smaller than those described for the isolation of adult bovine glomeruli and tubules (10). Tubules, isolated at 98% purity on sieve # 400, were stored at −80°C for future use.

Isolation of tubular basement membranes. TBM was isolated using a slight modification of the detergent extraction technique by Carlson et al. (11). Briefly, cells were lysed in a large (100:1) volume of 5 mM Tris-HCl, 0.02% sodium azide, 1 mM EDTA, 1 mM *N*-ethylmaleimide (NEM), 1 mM PMSF, pH 7.4, at 4°C overnight with constant stirring. Crude TBM was pelleted (3,000 rpm for 10 min), washed once with a solution of PBS, 0.02% sodium azide, 1 mM EDTA, 1 mM NEM, 1 mM PMSF, resuspended to 15 times the original tissue volume in 4% deoxycholic acid, 0.02% sodium azide, 1 mM EDTA, 1 mM NEM, 1 mM PMSF, and incubated 2.5 h at 37°C. After this detergent extraction, TBM was pelleted, washed 3 times in PBS, 0.02% sodium azide, resuspended to five times the original tissue volume in PBS, deoxyribonuclase A (50 Kunitz U/ml), 0.02% sodium azide, and incubated 1 h at 37°C. TBM was then washed three times in PBS, 0.02% sodium azide, 1 mM EDTA, 1 mM NEM, 1 mM PMSF, and aliquoted for immediate use.

Nonenzymatic glycosylation (NEG) of TBM. TBM was incubated for 2 wk at 37°C in solutions containing PBS, 1 mM EDTA, 1 mM PMSF, 1 mM NEM, 0.02% sodium azide, and one of the following: 1 M glucose, 1 M ribitol, or no sugar. Solutions were degassed under vacuum for 2 h to remove dissolved O_2 and then bubbled with argon to saturate with inert gas. Approximately 500 mg of pelleted TBM (equivalent to 33 mg lyophylized TBM) was resuspended in 50 ml of each of the respective solutions. Due to the limited buffering capacity of PBS, the pH of all samples had declined equivalently from 7.4 to 6.6 by the end of incubation. The TBM was pelleted (3,000 rpm for 10 min), washed three times with deionized water, and immediately processed for LV-SEM examination, SDS-PAGE, or fluorometric analysis.

Solubilization of TBM for SDS-PAGE and fluorometry. Because BM are highly crosslinked structures, solubilization was required before SDS-PAGE or fluorometric analysis could be performed.

Samples for SDS-PAGE analysis were digested with either collagenase or pepsin, or extracted in the absence of enzymatic digestion using a combination of denaturing and reducing agents. For digestion with collagenase, ~ 75 mg of pelleted TBM from each sample (equivalent to 5 mg lyophilized TBM) was resuspended with 1 ml of 50 μg/ml collagenase (CLSPA; Worthington Biochemical Corp., Freehold, NJ) in 50 mM Tris, 0.2 M NaCl, 2 mM $CaCl_2$, pH 7.4 (1:100 enzyme to substrate ratio), and incubated for 18 h at 37°C. For digestion with pepsin, 75 mg of pelleted TBM was resuspended in 1 ml of 25 μg/ml pepsin in 0.1 M acetic acid (1:200 enzyme to substrate ratio) and incubated for 18 h at 25°C. For extraction in the absence of any enzymatic digestion, ~ 225 mg of pelleted TBM from each sample (equivalent to 15 mg of lyophilized TBM) was resuspended in 3 ml of PBS, 5 M urea, 1% SDS, 4% 2-mercaptoethanol, pH 7.4, and incubated with constant shaking for 18 h at 60°C. In each separate approach, nonsolubilized material was pelleted by centrifugation (2,000 rpm for 2 min). The concentration of solubilized protein in the supernatant was determined for each sample using the method of Waddell (12). In the case of the nonenzymatically extracted material, this was performed after extensive dialysis with PBS, 2 M urea, 10 mM 2-mercaptoethanol, pH 7.4. Equivalent amounts of each TBM extract were then analyzed by SDS-PAGE.

Samples for fluorometric analysis were digested extensively by sequential treatment with collagenase and pepsin. TBM from each sample was resuspended with bacterial collagenase in 50 mM Tris, 0.2 M NaCl, 2 mM $CaCl_2$, pH 7.4, at a 1:100 enzyme to substrate ratio and incubated for 18 h at 37°C. At the end of incubation, samples were centrifuged at 70,000 rpm for 6 h. The pellet was resuspended with pepsin in 0.1 M acetic acid and 0.02% sodium azide at a 1:150 enzyme-to-substrate ratio and incubated for 36 h at 37°C with intermittent mixing by sonication. At the end of the incubation period, nonsolubilized material was pelleted by centrifugation (2,000 rpm for 2 min) and the supernatant was used for fluorometric analysis.

SDS-PAGE. Samples for SDS-PAGE were reduced and electrophoretically separated on 2–15% gradient separating gels according to the methods of Laemmli (13). Gels were stained with Coomassie blue, dried with BioGelWrap (BioDesign Inc., Carmel, New York), and analyzed densitometrically using a transmittance/reflectance scanning densitometer (model GS 300; Hoefer Scientific Instruments, San Francisco, CA) interfaced with an Apple IIe computer.

Fluorometric analysis. Fluorescence of previously solubilized TBM samples was measured at excitation/emission wavelengths of 335/385 nm and 360/460 nm. These wavelengths are known to detect various glycation-induced adducts, including pentosidine (14). Readings were obtained with a spectrofluorometer (Turner model 430; Unipath, Mountain View, CA) using a sample manipulated in parallel but containing only enzymes as a blank. Values were corrected for protein concentration as determined by the method of Waddell (12) and expressed as a percent of the negative control.

LV-SEM. Following incubation, suspensions of washed TBM from each sample were transferred to poly-L-lysine coated glass chips and processed for LV-SEM. Briefly, 5 mm × 10 mm glass chips were cut from standard microscope slides using a diamond-tipped pencil. After cleaning with sequential detergent, deionized water, acetone, and ethanol washes, 50 μl of a solution containing 100 μg/ml poly-L-lysine (M_r = 100,000) in PBS was pipetted onto the surface of each chip and incubated at room temperature for 1 h. The chips were then rinsed with deionized water and 50 μl of the various TBM samples suspended in PBS, 0.02% sodium azide, 1 mM EDTA, 1 mM NEM, and 1 mM PMSF were pipetted onto the poly-L-lysine coated glass surfaces and incubated for 1 h at 4°C. The chips were gently washed with PBS and adherent TBM were lightly fixed with 4% EM grade paraformaldehyde in PBS for 2 h at 4°C (4 ml fixative/6–8 chips). After fixation, the samples were rinsed thoroughly with deionized water, dehydrated in a graded series of increasing ethanol concentrations, and dried at critical point (Samdri-708A; Tousimis Research Corp., Rockville, MA). Dried samples were mounted on a 45° planetary rotating/tilting stage and coated with ~ 10 Å platinum using an ion beam microsputter system (model 705; VCR Group, Inc., San Francisco, CA) at 10 kV and 4 mA for 6 min (15). Coated samples were stored in a desiccated chamber before examination with a high resolution LV-SEM (Hitachi; S-900; Nisser Sangyo America, Ltd., Mountain View, CA) operating at an accelerating voltage of 2 kV (15).

A method of systematic field selection and photography was developed to assure the consistency and reproducibility of images. First, samples were surveyed at a magnification of 1,000 to identify flattened

areas of tubules that were undistorted and apparently adherent to the glass chip. Magnification was then increased to 5,000, the flattened areas were centered in the field, and magnification was increased to 80,000 to allow for a detailed examination of the underlying structure. Fields were photographed with Polaroid film type 52. Brightness and contrast were adjusted automatically, and film development time was kept constant to assure reproducibility among images. Stereo-paired photographs were taken of most regions to assure that fields selected for analysis were flat with respect to the plane of the photographic film.

Image analysis. Representative images from ribitol- and glucose-treated TBM were inputted through an MTI Series 68 CCD array camera to an image processor (model 75; International Image Systems, Milpitas, CA). The image processor was interfaced with a minicomputer (model 5700; Concurrent Computer Corporation Westford, MA), which ran System 600 image processing software (International Image Systems) under the UNIX operating system. Digitized images were converted to gray-scale histograms in which black was assigned a value of 0; white, 256; and shades of gray, intermediate values. The percentages of image surface area occupied by regions darker than specific levels of grayness were determined using software developed by R. Carter Carpenter of the University of Minnesota Biomedical Image Processing Laboratory. The obtained values were compared using a two-tailed Student's *t* test.

An additional image analysis technique was used to more specifically compare the apparent number and size of individual openings. Images of ribitol- and glucose-treated TBM were enlarged to a magnification of 104,000. "Openings" in the TBM structure, defined as strictly as possible to represent dark regions of the image that contained no apparent detail or structure underneath, were manually outlined and darkened to facilitate selective detection and measurement using the image analysis hardware and software described previously. In order to avoid bias, the identification of openings was performed independently by two observers, one of them unfamiliar with the research project. The total amounts of image surface area occupied by openings were determined. Also, the number of openings and amount of image surface area occupied by openings of specific sizes was determined for each image and presented according to opening diameter, which was calculated assuming each had an approximately circular shape. The results, expressed as mean±SD, were compared using a two-tailed Student's *t* test.

Results

It is well established that incubation with reducing sugars leads to the generation of glycated and crosslinked proteins in vitro (6, 16–19). In order to document such changes in our experiments, TBM, which had been incubated as described in Methods, was solubilized and examined by electrophoresis and fluorometric analysis. Three lines of evidence suggest the formation of crosslinks. First, glucose-treated TBM was noted to be less susceptible to enzymatic degradation and chemical extraction than ribitol-treated control TBM, as determined by the amount of protein solubilized and the volume of the pellets that remained after each treatment (data not shown). Second, densitometric analysis of electrophoretic profiles of TBM extracts detected more high molecular weight material in glucose-treated samples compared to control. These findings are typical for tissues that have become crosslinked as a result of glycation (17, 18, 20–22). Finally, fluorometric analysis detected increased fluorescence in glucose-treated TBM compared to ribitol-treated TBM at two different wavelengths that detect glycation-generated crosslinks (Fig. 1). Although fluorescent crosslinks are thought to represent only a certain percentage of the total population of crosslinks that form as a result of glycation, they are useful biomarkers for the larger population and provide a sensitive way to access crosslink formation (23). As can be seen in Fig. 1, glucose-treated TBM demonstrated a 72% increase in fluorescence at 335/385 nm when compared to untreated controls. This wavelength is optimal for the detection of pentosidine crosslinks (14). Additionally, a 67% increase in fluorescence was observed at 360/460 nm, which is considered optimal for the detection of other crosslinks (14). TBM treated with ribitol, a nonreducing sugar, remained at a baseline level of fluorescence, confirming that this sugar did not participate in the process of NEG and crosslink formation.

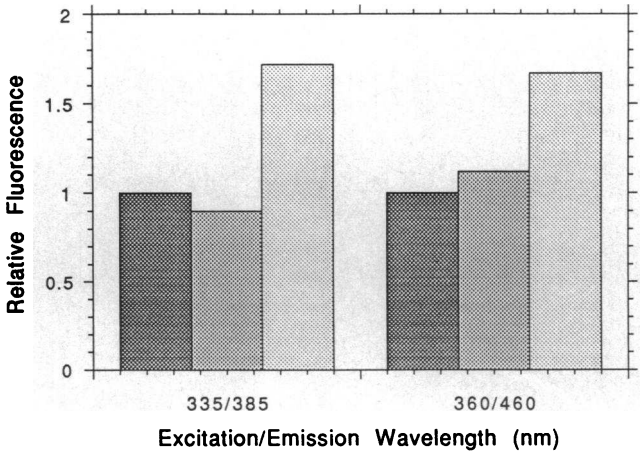

Figure 1. Fluorometric analysis of control and glycated TBM. TBM previously incubated with either no sugar (▨), 1 M ribitol (▨), or 1 M glucose (▨) for 2 wk at 37°C was solubilized using sequential digestion with collagenase and pepsin. Fluorescence was measured at excitation/emission wavelengths of 335/385 and 360/460 nm, respectively, which detect glycation-induced protein crosslinks. Values were corrected for the protein concentration of each sample and expressed as a percentage of untreated control.

It was possible that different amounts and types of BM components were extracted from the TBM by the various incubation solutions resulting in morphological changes unrelated to NEG and crosslinking. To address this issue, TBM were pelleted at the end of the 2-wk period of incubation, and the solutions used for incubation were analyzed for differences in protein content using the method of Waddell et al. and SDS-PAGE. No differences were detected in the amount or type of components extracted by the solutions containing ribitol vs. glucose (data not shown). In addition, ribitol treatment of TBM should control for possible nonspecific effects of the high tonicity and high sugar concentration of the glycation solution on TBM morphology.

LV-SEM examination of the acellular TBM at a magnification of 1,000 revealed collapsed, thin-walled tubular structures (Fig. 2). Since most TBM maintained their tubelike structure, the interstitial side of the TBM was the principal surface visible, and only small amounts of luminal surface were occasionally exposed at the sheared ends. Regions of the interstitial surface that appeared to be flattened, undistorted, and adjacent to the surface of the glass chip were selected for examination at higher power. These regions consistently generated images that were parallel with respect to the plane of the photographic film as determined by stereoscopy. In addition, since these regions were a uniform distance from the secondary electron detector of the LV-SEM, a consistent factor of magnification among images was assured.

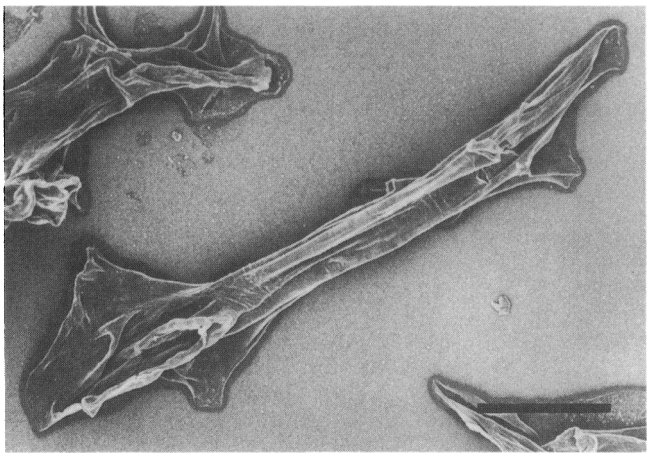

Figure 2. LV-SEM image of isolated acellular TBM. Examination of TBM at low magnification revealed collapsed, thin-walled tubular structures. Flattened regions of the interstitial surface were targeted for further examination at high magnification. Bar, 20 μm.

LV-SEM analysis at higher power revealed a complex meshwork of interconnecting strands of BM material with intervening openings of different sizes. The structure was comparable to that recently described by Hironaka et al. using similarly prepared TBM and LV-SEM (24). Because of the complexity of the multilayered three-dimensional network, it was difficult to identify a distinctive pattern in the structure of the lattice (Figs. 3 and 4). In some instances, however, semi-regular structures could be visualized in which strands of material appeared to radiate from a central hub into various planes of the lattice, occasionally having the appearance of a pentagonal or hexagonal wheel with spokes (Fig. 3).

Following glycation, there were distinctive changes in the appearance of TBM ultrastructure. Initial visual comparison of LV-SEM images suggested that more surface area was occupied by openings and that some openings were enlarged in glucose-treated TBM compared to the control. In addition, there appeared to be more frequent clustering of TBM material in glucose-treated TBM, particularly in regions adjacent to enlarged openings. Differences between control and glycated TBM were more apparent when the structures were viewed in three dimensions using stereo-paired images: representative fields are shown in Fig. 4, *A* and *B* for ribitol-treated TBM and in Fig. 4, *C* and *D* for glucose-treated TBM.

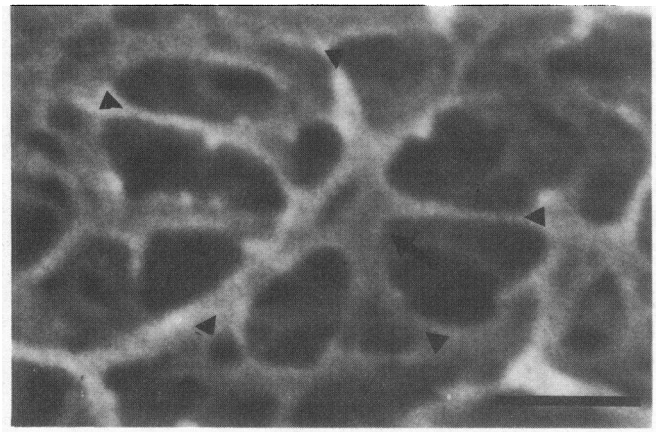

Figure 3. LV-SEM image of a selected area of the TBM at very high magnification. A complex meshwork of interconnecting strands of BM material with intervening openings of different sizes was revealed by LV-SEM. Occasionally, semi-regular structures could be identified in which strands of material (*arrowheads*) appeared to radiate from a central hub (*arrow*) into various planes of the lattice, producing the appearance of a pentagonal or hexagonal wheel with spokes. Bar, 50 nm.

In order to statistically evaluate the area occupied by openings in the SEM images of control and glycated TBM, computer-aided analysis was performed. First, the amount of image surface area occupied by dark regions, which correspond to open spaces in the TBM structure, was quantitated for glucose- and ribitol-treated samples. For this analysis, representative images were digitized and the amount of image surface area occupied by various shades of gray was determined. As can be seen in Fig. 5, the gray-scale distribution for images of glucose-treated TBM was skewed toward darker shades of gray when compared to the distribution for images of the control. These differences were statistically significant at gray-scale values between 0 and 96, which represented the darkest spots in the SEM images and therefore corresponded to areas visualized as openings. These data indicate that more surface area was occupied by openings in images from glucose-treated TBM compared to images from the control.

An additional method of analysis was performed to assess the amount of surface area occupied by openings in images of glycated and control TBM. For this technique, individual openings were outlined and darkened to allow for selective detection in the digitized images used for computer analysis. Images from glucose-treated TBM were found to have 58% more surface area occupied by openings than images from ribitol-treated control TBM (13.34±0.64% vs. 8.44±1.18%, $P < 0.001$). The obtained data were comparable to those generated with the previous image analysis technique in which dark shades of gray (gray levels of $\sim$ 82) were significantly increased in images of glycated TBM.

This increase in the amount of image surface area occupied by openings after TBM glycation could be due to an increase in the number and/or the size of individual openings. Using the second image analysis technique, the amount of image surface area occupied by openings of various sizes was determined and presented according to opening diameter (Fig. 6 *A*). This type of analysis indicated that there was no significant difference in the surface area occupied by "small" openings with diameters < 12.5 nm in images of control and glycated TBM. However, "large" openings with diameters >12.5 nm occupied significantly more surface area in the images of glycated TBM. This was due to a small and similarly significant increase in the number of large diameter openings (data not shown).

Discussion

In this report we describe: (*a*) the three-dimensional appearance of isolated TBM as revealed at extremely high resolution by LV-SEM, and (*b*) biochemical and morphological changes in TBM after incubation in the presence of glucose.

The selection of TBM as a model BM in our system is based on several factors. TBM can be easily isolated in large quantities and at high (98%) purity and has a relatively consistent and homogeneous appearance by LV-SEM. This in contrast to

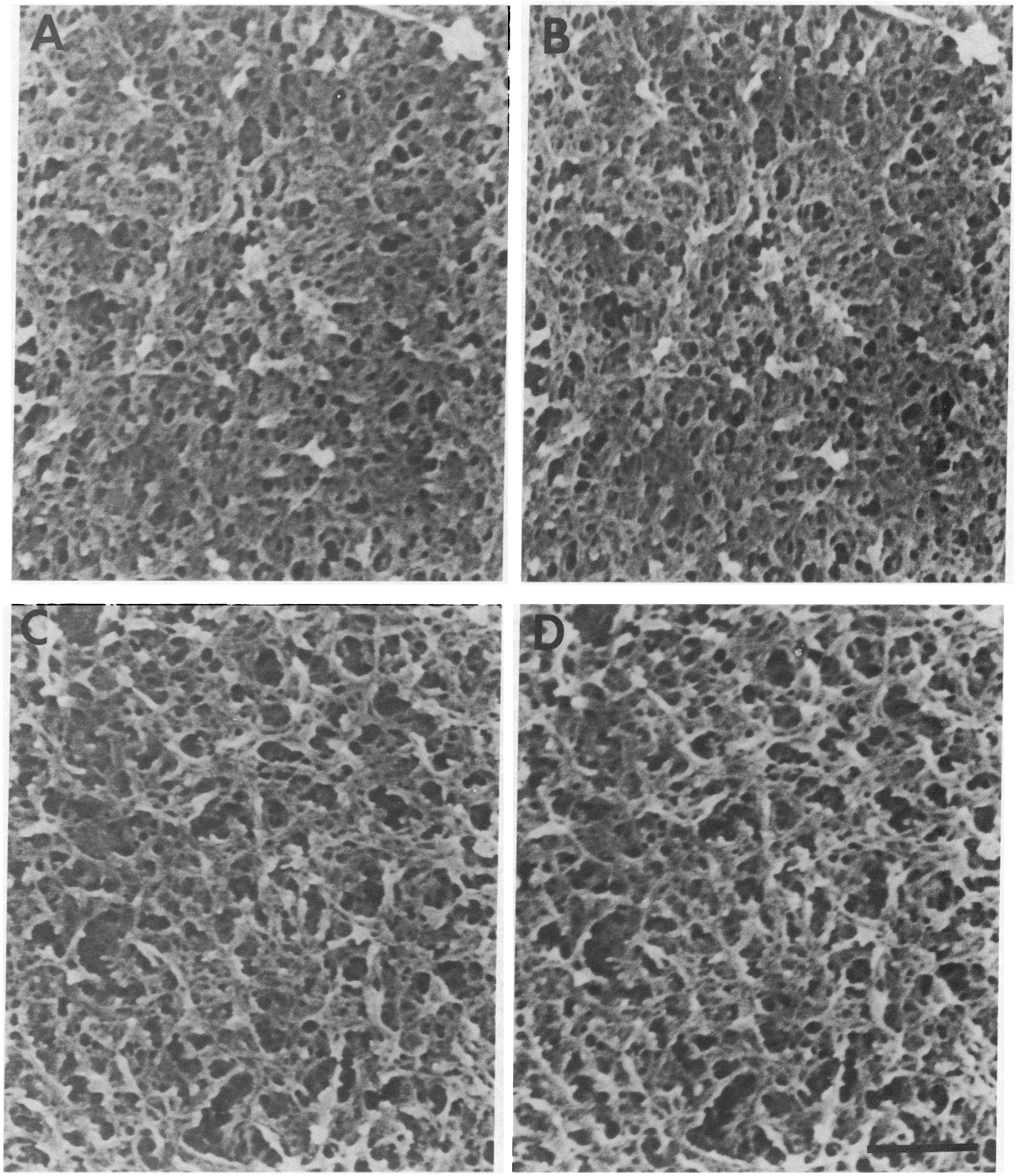

Figure 4. Stereo-paired LV-SEM images of control and glycated TBM. Representative images of ribitol-treated (*A* and *B*) and glucose-treated (*C* and *D*) TBM revealed strands of material of varying thickness intertwined to form a quasi-regular network with openings of various sizes. Openings appear to occupy a greater proportion of image surface area, and some of these openings appear larger in the glycated matrix compared to the control. Bar, 250 nm.

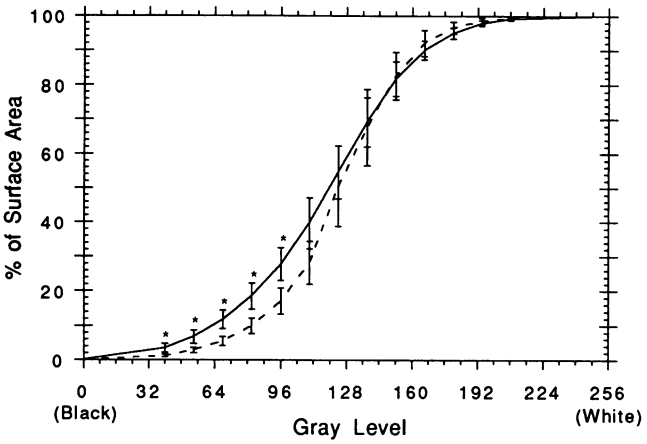

Figure 5. Comparison of gray-scale distribution from images of control and glycated TBM. The percentage of image surface area composed of regions darker than a series of specific shades of gray was determined using computer-aided image analysis of 15 images each of either ribitol-treated (*broken line*) or glucose-treated (*solid line*) TBM. Images of glycated TBM had significantly more surface area composed of dark shades of gray and black (gray-scale values between 0 and 96), which correspond to openings in the matrix. Results are expressed as mean±SD (*$P < 0.001$).

GBM, which unavoidably contains mesangial matrix and has a more heterogeneous appearance. In addition, the structure of TBM is representative of other BM (24). Also, TBM along with GBM has been described to become diffusely thickened in diabetic patients (25). Finally, in physiological studies, TBM and GBM have similar dextran sieving properties (26).

The methodology for TBM preparation and ultra high resolution LV-SEM examination used here consistently resulted in images of a characteristic lattice-like BM structure. Thin strands of material were interlaced to form a fine meshwork

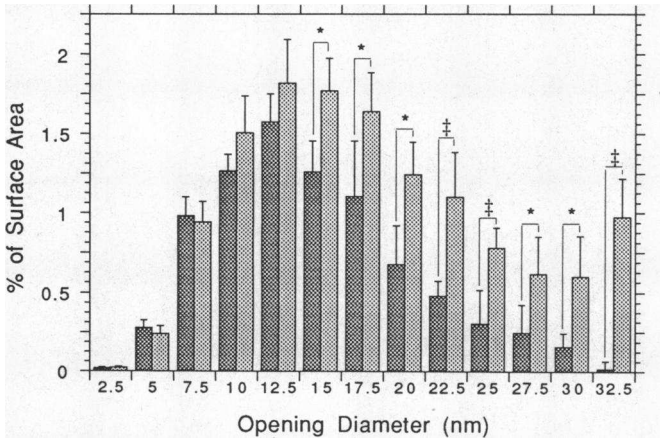

Figure 6. Percentage of image surface area occupied by openings of specific sizes. "Openings" in the TBM structure, defined as dark regions of the image that contained no apparent detail or structure, were darkened to facilitate selective detection and measurement in digitized images used for computer analysis. The percentage of image surface area occupied by openings was presented according to opening diameter as calculated, assuming each had an approximately circular shape. Values are expressed as the mean±SD from six images each of ribitol-treated (▨) or glucose-treated (▤) TBM (*$P < 0.02$, ‡$P < 0.001$).

that had openings of varying sizes. Although it was difficult to identify a basic subunit structure, several strands of BM material could frequently be seen emanating from a common point into different planes of the complex meshwork, occasionally giving the appearance of a pentagonal or hexagonal wheel with spokes. These structures, however, were not as prevalent or regular as those in published images of the BM of corneal epithelium (27). The lattice visualized in these minimally extracted TBM was also more complex and denser than the structure of heavily extracted parietal basement membrane (which should be composed primarily of tIV) as revealed by etching and transmission electron microscopy (28, 29). In addition, TBM structure demonstrated in this report was more detailed and discrete than that of several previous reports that made use of SEM (30–32) and transmission electron microscopy (33–37) to analyze the structure of kidney-derived BM. Dissimilarities in the appearance of BM among reports is probably due to differences in the source and preparation of the tissues as well as the methods of morphological analysis. In contrast, the TBM structure presented here is comparable to that recently published by Hironaka et al. using similar methods for both tissue preparation and ultra high resolution LV-SEM analysis (24).

In order to assess the effect of NEG on TBM structure, we have used a system of "accelerated glycation." In situ, most BM components turn over slowly and apparently take several years to become substantially modified in the presence of hyperglycemia (6–15 mM glucose) (22, 38). Our system was designed to produce similar changes in a much shorter time interval (14 d): therefore, it was imperative to use high glucose concentrations. Glycation-induced modifications and extensive crosslink formation were demonstrated in the glucose-treated TBM by detecting: (*a*) decreased susceptibility to enzymatic digestion and chemical extraction, (*b*) increased high molecular weight material with low electrophoretic mobility in samples of solubilized TBM, and (*c*) increased fluorescence at wavelengths known to detect glycation-induced crosslink products when compared to ribitol-treated TBM. The observed increase in crosslink-associated fluorescence for glycated TBM under our experimental conditions (~ 70%) was comparable to the relative increase in fluorescence seen for samples of skin collagen from diabetic patients compared to age-matched nondiabetic counterparts (39).

Glycation resulted in distinct morphological changes in TBM ultrastructure. These included an increase in the amount of TBM surface area occupied by openings as demonstrated using two different methods of image analysis. This was due to an increase in the number of "large" openings (diameter > 12.5 nm) in the glycated TBM, while the number of "small" openings remained unchanged. The openings examined in this report represent only a portion of possibly very tortuous and complex "pores" through which a molecule must travel in order to traverse the entire thickness of the sievelike BM. Since the size of a "pore" is apparently limited by the diameter of the smallest opening that occurs along its path, a substantial increase in the amount of large openings could correspond to only a modest increase in the overall porosity of the entire BM.

To our knowledge, we are the first to provide morphological evidence for the existence of more and larger openings in BM chemically modified by glucose (40–42). If similar changes were to occur in BM structures in vivo, they could play a role in the development of changes in glomerular permselectivity such

as those seen in diabetic nephropathy (43). Several physiological studies in humans, using macromolecules of variable size, charge, and shape, have provided evidence that loss of size selectivity through the formation of a small number of larger pores in the filtering sieve of the kidney could account for the loss of permselectivity in diabetes (2). Our morphological observations and measurements strongly support the above-mentioned physiological findings, in that we confirmed with high resolution LV-SEM the existence of enlarged openings in glycated BM. Furthermore, our observations indicate that glycation and glucose-induced crosslink adducts could be causally related with the appearance of enlarged openings. Although the exact mechanism is not known, crosslinking may lead to clustering of BM components causing alterations in the normal basement membrane ultrastructure.

These studies were designed to examine the effect of one factor, the nonenzymatic glycosylation of matrix proteins, on one component of the vascular wall, the basement membrane. Other factors related to the diabetic condition may also be involved in the alteration of vascular wall structure and function. In addition, the basement membrane is only part of the filtration unit, which also includes the endothelial layer and epithelial layer with podocytes and filtration slits. Therefore, changes in these structures could be of importance in determining the permeability properties of the diabetic glomerulus.

In view of our findings, it will be of interest to use this in vitro system to examine the filtration properties of control and glycated BM to determine if the observed structural changes have an effect on BM permeability. It will also be of interest to examine BM isolated from kidneys of patients with diabetic nephropathy, using the morphological approach described in this report to compare the appearance of BM diabetically modified in vivo with that of in vitro glycated BM.

Acknowledgments

We thank Dr. Vincent Monnier for helpful suggestions on the use of nonreducing sugars, Dr. Theodore Oegema for the use of the spectrofluorometer, and Dr. Stan Erlandsen for the use of the LV-SEM. We also thank Chris Frethem for his advice and technical assistance with the LV-SEM; R. Carter Carpenter of the University of Minnesota Biomedical Image Processing Laboratory for his advice and assistance with the computer-aided analysis of LV-SEM images; and Jennifer Thull for useful discussion and advice during the preparation of the manuscript.

This work was supported by the National Institutes of Health under the auspices of the National Institute of Arthritis, Diabetes, Digestive and Kidney Diseases grants 39216 and 43574 (to E. C. Tsilibary) and 43564 (to A. S. Charonis); and by grants from the Juvenile Diabetes Foundation International (to E. C. Tsilibary), the American Diabetes Association Minnesota Affiliate (to A. S. Charonis), the American Diabetes Association (to E. C. Tsilibary), the American Heart Association Minnesota Affiliate (to A. S. Charonis and E. C. Tsilibary), and the National Kidney Foundation of the Upper Midwest (to S. S. Anderson).

References

1. Timpl, R., and D. Dziadek. 1986. Structure, development, and molecular pathology of basement membranes. *Int. Rev. Exp. Pathol.* 29:1–112.

2. Myers, B. D. 1990. Pathophysiology of proteinuria in diabetic glomerular disease. *J. Hypertens.* 8:S41-S46.

3. Østerby, R., H.-H. Parving, E. Hommel, H. E. Jørgensen, and H. Løkkegaard. 1990. Glomerular structure and function in diabetic nephropathy: early to advanced changes. *Diabetes* 39:1057–1063.

4. Monnier, V. M. 1989. Toward a Maillard reaction theory of aging. *Prog. Clin. Biol. Res.* 304:1–22.

5. Njoroge, F. G., and V. M. Monnier. 1989. The chemistry of the Maillard reaction under physiological conditions: a review. *Prog. Clin. Biol. Res.* 304:85–107.

6. Charonis, A. S., and E. C. Tsilibary. 1992. Structural and functional changes in laminin and type IV collagen after nonenzymatic glycosylation. *Diabetes.* 41(Suppl. 2):49–51.

7. Charonis, A. S., L. A. Reger, J. E. Dege, K. Kouzi-Koliakos, L. T. Furcht, R. M. Wohlhueter, and E. C. Tsilibary. 1990. Laminin alterations after in vitro nonenzymatic glycosylation. *Diabetes.* 39:807–814.

8. Haitoglou, C. S., E. C. Tsilibary, M. Brownlee, and A. S. Charonis. 1992. The effect of non-enzymatic glucosylation on self-assembly and cell binding properties of type IV collagen. *J. Biol. Chem.* 267:12404–12407.

9. Tsilibary, E. C., A. S. Charonis, L. A. Reger, R. M. Wohlhueter, and L. T. Furcht. 1988. The effect of nonenzymatic glucosylation on the binding of the main noncollagenous NC1 domain to type IV collagen. *J. Biol. Chem.* 263:4302–4308.

10. Butkowski, R. J., and S. Hagen. 1990. A method for preparation of renal tubular basement membrane. *Connect. Tissue Res.* 25:121–130.

11. Carlson, E. C., K. Brendel, J. T. Hjelle, and E. Meezan. 1978. Ultrastructural and biochemical analyses of isolated basement membranes from kidney glomruli and tubules and brain and retinal microvessels. *J. Ultrastruct. Res.* 62:26–53.

12. Waddell, N. J. 1956. A simple ultraviolet spectrophotometric method for the determination of protein. *J. Lab. Clin. Med.* 48:311–314.

13. Laemmli, U. K. 1970. Cleavage of structured proteins during assembly of the head of bacteriophage T_4. *Nature (Lond.).* 227:680–685.

14. Sell, D. R., and V. M. Monnier. 1989. Isolation, purification, and partial characterization of novel fluorophores from aging human insoluable collagen-rich tissue. *Connect. Tissue Res.* 19:77–92.

15. Pawley, J. B., and S. L. Erlandsen. 1989. The case for low voltage high resolution scanning electron microscopy of biological samples. *Scanning Microsc.* 3:163–178.

16. Dyer, D. G., J. A. Blackledge, S. R. Thorpe, and J. W. Baynes. 1991. Formation of pentosidine during nonenzymatic browning of proteins by glucose: identification of glucose and other carbohydrates as possible precursors of pentosidine *in vivo. J. Biol. Chem.* 266:11654–11660.

17. Kent, M. J. C., N. D. Light, and A. J. Bailey. 1985. Evidence for glucose-mediated covalent cross-linking of collagen after glycosylation *in vitro. Biochem. J.* 225:745–752.

18. Tanaka, S., G. Avigad, E. F. Eikenberry, and B. Brodsky. 1988. Isolation and partial characterization of collagen chains dimerized by sugar-derived cross-links. *J. Biol. Chem.* 263:17650–17657.

19. Hayase, F., R. H. Nagaraj, S. Miyata, F. G. Njorge, and V. M. Monnier. 1989. Aging of proteins: immunological detection of a glucose-derived pyrrole formed during Maillard reaction *in vivo. J. Biol. Chem.* 263:3758–3764.

20. Kohn, R. R., and S. L. Schnider. 1982. Glucosylation of human collagen. *Diabetes.* 31:47–51.

21. Lubec, G., and A. Pollak. 1980. Reduced susceptibility of nonenzymatically glycosylated glomerular basement membrane to proteases: is thickening of diabetic glomerular basement membranes due to reduced proteolytic degradation? *Renal Physiol.* 3:4–8.

22. Trüeb, B., R. Fluckiger, and K. H. Winterhalter. 1984. Nonenzymatic glycosylation of basement membrane collagen in diabetes mellitus. *Collagen Relat. Res.* 4:239–251.

23. Baynes, J. S. 1991. Role of oxidative stress in development of complications in diabetes. *Diabetes.* 40:405–412.

24. Hironaka, K., H. Makino, Y. Yamasaki, and Z. Ota. 1993. Renal basement membranes by ultrahigh resolution scanning electron microscopy. *Kidney Int.* 43:334–354.

25. Steffes, M. W., D. E. R. Sutherland, F. C. Goetz, S. S. Rich, and S. M. Mauer. 1985. Studies of kidney and muscle biopsy specimens from identical twins discordant for type I diabetes mellitus. *N. Engl. J. Med.* 312:1282–1287.

26. Moran, M. S., and B. D. Myers. 1985. Pathophysiology of protracted acute renal failure in man. *J. Clin. Invest.* 76:1440–1448.

27. Sawada, H. 1982. The fine structure of the bovine Descemet's membrane with special reference to biochemical nature. *Cell Tissue Res.* 226:241–255.

28. Inoue, S., C. P. LeBlond, and G. W. Laurie. 1983. Ultrastructure of Reichert's membrane, a multilayered basement membrane in the parietal wall of the rat yolk sack. *J. Cell Biol.* 97:1524–1537.

29. Yurchenco, P. D., and G. C. Ruben. 1987. Basement membrane structure *in situ:* evidence for lateral association in the type IV collagen network. *J. Cell Biol.* 105:2559–2568.

30. Makino, H. 1988. Three-dimentional ultrastructure of rat acellular glomerulus by scanning electron microscopy. *J. Electron Microsc.* 37:294–304.

31. Shirato, I., Y. Tomino, H. Koide, and T. Sakai. 1991. Fine structure of the glomerular basement membrane of the rat kidney visualized by high-resolution scanning electron microscopy. *Cell Tissue Res.* 266:1–10.

32. Yamasaki, Y., H. Makino, K. Hironaka, Y. Hayashi, K. Shikata, and Z. Ota. 1990. Three-dimensional architecture of rat glomerular basement mem-

brane by ultra-high resolution scanning electron microscopy. *Acta Med. Okayama* 44:333–335.

33. Carlson, E. C., E. Meezan, K. Brendel, and M. C. Kenney. 1981. Ultrastructural analyses of control and enzyme-treated isolated renal basement membranes. *Anat. Rec.* 200:421–436.

34. Kubosawa, H., and Y. Kondo. 1985. Ultrastructural organization of the glomerular basement membrane as revealed by deep-etch replica method. *Cell Tissue Res.* 242:33–39.

35. Laurie, G. W., C. P. LeBlond, S. Inoue, G. R. Martin, and A. Chung. 1984. Fine structure of the glomerular basement membrane and immunolocalization of five basement membrane components to the lamina densa (basal lamina) and its extensions in both glomeruli and tubules of the rat kidney. *Am. J. Anat.* 169:463–481.

36. Ota, Z., H. Makino, Y. Takaya, and T. Ofuji, 1980. Molecular sieve in renal glomerular and tubular basement membrane as revealed by electron microscopy. *Renal Physiol.* 3:317–323.

37. Shikata, K., H. Makino, A. Ichiyasu, and Z. Ota. 1990. Three-dimensional meshwork structure of glomerular basement membrane revealed by chemical treatment. *J. Electron. Microsc.* 39:182–185.

38. Cohen, M. P., E. Urdanivia, M. Surma, and V. W. Wu. 1980. Increased glycosylation of glomerular basement membrane collagen in diabetes. *Biochem. Biophys. Res. Commun.* 95:765–769.

39. Monnier, V. M., V. Vishwanath, K. E. Frank, C. A. Elmets, P. Dauchot, and R. R. Kohn. 1986. Relation between complications of type I diabetes mellitus and collagen-linked fluorescence. *N. Engl. J. Med.* 314:403–408.

40. Anderson, S. S., A. S. Charonis, and E. C. Tsilibary. 1991. Diabetic modification of kidney basement membrane ultrastructure and altered interaction with mesangial cells. *J. Cell Biol.* 115:438*a*. (Abstr.)

41. Anderson, S. S., E. C. Tsilibary, and A. S. Charonis. 1992. Nonenzymatic glucosylation induced structural changes of kidney basement membranes. *Diabetes.* 41:292. (Abstr.)

42. Anderson, S. S., A. S. Charonis, Y. Kim, and E. C. Tsilibary. 1992. Altered basement membrane structure and interaction with kidney mesangial cells following nonenzymatic glycosylation. *Kidney Int.* 3:625. (Abstr.)

43. Myers, B. D., J. A. Winetz, F. Chui, and A. S. Michaels. 1982. Mechanisms of proteinuria in diabetic nephropathy: a study of glomerular barrier function. *Kidney Int.* 21:633–641.